JOURNAL OF GEOPHYSICAL RESEARCH, VOL. 102, NO. B6, PAGES 12,109–12,121, JUNE 10, 1997

A model for the formation of transient event plumes above mid-ocean ridge hydrothermal systems

William S. D. Wilcock

School of Oceanography, University of Washington, Seattle

Abstract. Event plumes (or megaplumes) are ephemeral bodies of anomalously warm water which form in the water column above mid-ocean ridges as the result of the catastrophic release of large volumes of hydrothermal fluid. During the formation of the largest event plumes, heat fluxes increase to at least 100 times those of a typical high-temperature vent field. Recent observations reveal a strong association between event plumes and diking-eruptive events. It has previously been suggested that event plumes are the result of increased fluxes throughout hydrothermal systems following a large increase in the permeability of a critical region. In this paper, an alternative model is explored whereby the volume of fluid expelled is not balanced by increased downflow but rather by the expansion of fluids near the base of the system. For most geologically plausible patterns of hydrothermal circulation, the fracturing and faulting associated with a diking event will result in a much larger decrease in the flow resistance of the upflow zone than the downflow zone. To balance fluxes, the pressure must decrease throughout the system. There is considerable evidence that the fluids near the base of mid-ocean ridge hydrothermal convection cells lie near the two-phase boundary for seawater and thus are very compressible. Simple calculations show that fluid expansion in a depressurized reaction zone can match the observed formation times and sizes of large event plumes only if the permeability of the upflow zone increases to very high values (~10^{-9}-10^{-10} m^2) and if the plume is underlain by a sizable reaction zone containing at least 0.01-0.2 km^3 of fluid at temperatures near the two-phase curve. Fluid expansion in a smaller reaction zone is a plausible mechanism to incorporate a component of mature hydrothermal fluid into event plumes whose heat content comes primarily from cooling lava flows. It may also be responsible for smaller event plumes or temporal fluctuations in chronic plumes which are not linked to volcanic eruptions but which follow tectonically or magmatically induced increases in permeability.

Introduction

The terms megaplume [*Baker et al.*, 1987] and event plume [*Baker*, 1994] were coined to describe the results of catastrophic releases of large volumes of hydrothermal fluid into the water column above mid-ocean ridges. The continuous discharge of fluids from high-temperature hydrothermal systems results in the formation of chronic plumes which typically rise about 100-300 m above the seafloor [*Baker*, 1994]. In contrast, event plumes are characterized by a rise height of about 1 km and their formation requires heat fluxes several orders of magnitude greater than those from steady state vent fields. Event plumes have been reported from the Juan de Fuca Ridge [*Baker et al.*, 1987, 1989, 1995; *Baker*, 1994], the Gorda Ridge [*Baker et al.*, 1996], and from back arc spreading centers [*Nojiri et al.*, 1989; *Gamo et al.*, 1993].

The first two event plumes [*Baker et al.*, 1987, 1989] were discovered in 1986 and 1987 near the Cleft segment of the Juan de Fuca Ridge (Figure 1). The plumes were disk-shaped with diameters of about 20 km, thicknesses of 500-700 m, and maximum potential temperature anomalies exceeding 0.2°C. After accounting for the entrainment of cold water, *Baker et al.* [1989] estimate the heat released to be 1.2 x 10^{17} and 0.6 x 10^{17} J for the 1986 and 1987 events, respectively. The physical and chemical characteristics of the 1986 plume lead *Baker et al.* [1989] to conclude that it formed very shortly before discovery by the release of ~0.1 km^3 of mature ~350°C hydrothermal fluid. By modeling the source as a linear fissure, *Baker et al.* [1989] show that the maximum rise height of 1 km requires a heat flux of 3.5 x 10^8 J s^{-1} per meter of source. For a fissure length of 200-2000 m, the 1986 plume would have formed in 20 to 2 days during which time the total heat flux would have been 100-1000 times the steady heat flux of 7 x 10^8 J s^{-1} estimated for the northern Cleft chronic plume [*Baker*, 1994]. Repeat Sea beam surveys and on-bottom camera observations show that a series of volcanic mounds erupted along a 20-km section of the northern Cleft segment between 1981 and 1987 [*Chadwick et al.*, 1991], lending circumstantial support to the hypothesis that event plumes are related to rifting events [*Baker et al.*, 1987, 1989]. Two smaller event plumes were also observed along the Cleft segment in 1987 and 1989 [*Baker*, 1994].

Irrefutable evidence for an association between large event plumes and diking was provided by the 1993 eruption on the CoAxial segment (Figure 2). Over a period of 2 days, epicenters from a seismic swarm on the northern flank of Axial seamount migrated 40 km to the north where seismicity continued intermittently for 3 weeks [*Dziak et al.*, 1995; *Fox et al.*, 1995; *Schreiner et al.*, 1995]. A small eruption was discovered at the end of a 7-km-long fissure, and both the fissure and the extrusion were venting warm water [*Embley et al.*,

Paper number 97JB00512.
0148-0227/97/97JB-00512$09.00

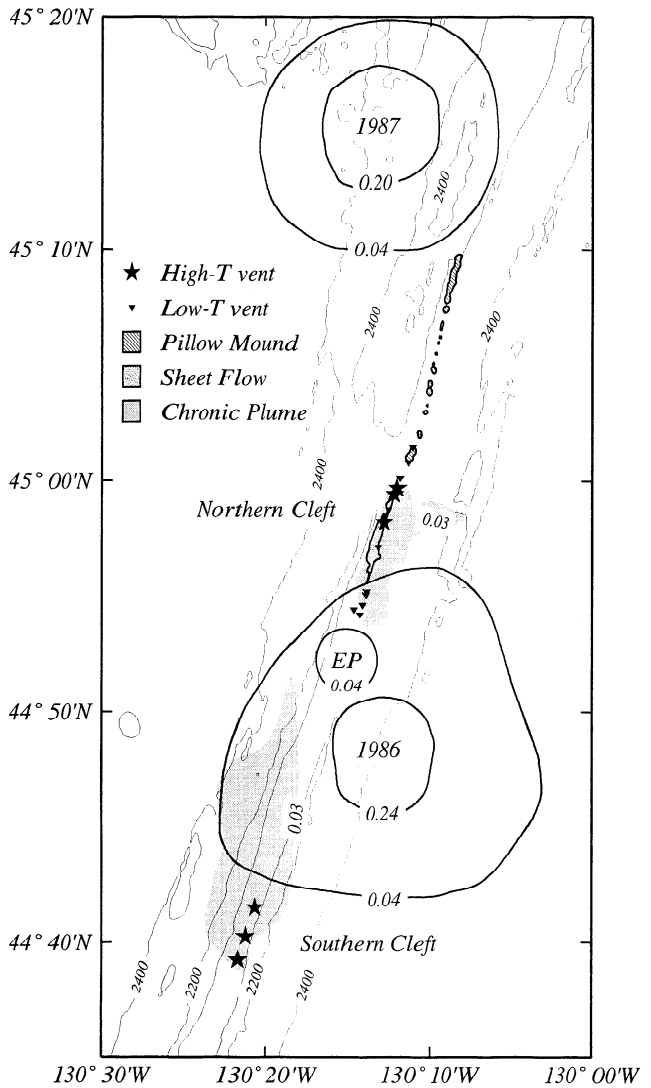

Figure 1. Simplified bathymetric map of the Cleft segment, contoured at 200 m intervals, showing the location of hydrothermal plumes and recent eruptions. Labeled contours of temperature anomalies in degrees Celsius delineate the positions of the 1986 and 1987 megaplumes [*Baker et al.*, 1989], the smaller 1989 event plume (EP) [*Baker*, 1994; *Massoth et al.*, 1994], and the chronic plumes (light shading) [*Baker*, 1994; *Massoth et al.*, 1994]. The locations of recent lava flows (stipled and striated with bold outlines) [*Chadwick and Embley*, 1994; *Embley and Chadwick*, 1994], high-temperature vents (stars) [*Embley et al.*, 1994], and representative sites of diffuse venting (triangles) [*Embley and Chadwick*, 1994] are also shown.

1995; *Chadwick et al.*, 1995]. Over a 3 week period following the onset of seismicity, water column studies detected at least three event plumes [*Baker et al.*, 1995] with diameters of 10 km, rise heights of nearly 1 km, and excess heat contents about one tenth those of the Cleft plumes. Numerical models suggest that each plume was discharged from a linear source in a matter of hours [*Lavelle*, 1995]. A tentative chronology [*Baker et al.*, 1995, *Massoth et al.*, 1995] requires that the plumes were emitted intermittently over a period of at least a week, and *Baker et al.* [1995] hypothesize that each plume was associated with a separate pulse of seismic swarm activity [*Dziak et al.*, 1995]. Most recently, an event plume was discovered in March 1996 above a fresh eruption on the Gorda Ridge [*Baker et al.*, 1996].

Chemically, the hydrothermal fluids which form event plumes are quite distinct from those of adjacent steady state systems. The 1986 Cleft event plume was characterized by lower Mn/Fe, SiO_2/heat, and Mn/heat ratios than an underlying chronic plume from the high-temperature North Cleft vent field [*Baker et al.*, 1987]. The ^{3}He/heat ratios in the event plume were 15 times lower than anomalously high ratios in the chronic plume [*Lupton et al.*, 1989]. The CoAxial event plumes were not underlain by a high-temperature vent field but showed similar chemical differences to a chronic plume formed by extensive diffuse venting [*Massoth et al.*, 1995, *Lupton et al.*, 1995]. The ^{3}He/heat ratios were on average 5 times lower in the event plumes than in the underlying plumes [*Lupton et al.*, 1995]. Thus the concentrations of magmatically derived volatiles and metals are much higher in the chronic plumes than the event plumes.

A number of models have been advanced to explain the formation of event plumes. *Baker et al.* [1987] first suggest that

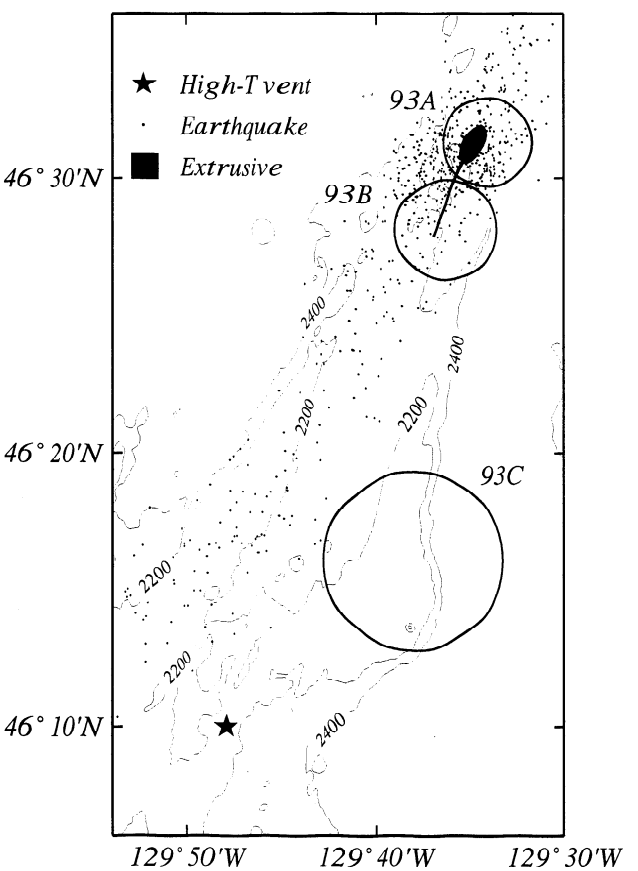

Figure 2. Simplified bathymetric map of the CoAxial segment, contoured at 200 m intervals, showing the configuration of the 1993 diking event. The map shows the location of the lava flow (solid fill) and a 7-km-long rift extending to the south (solid line) [*Embley et al.*, 1995], three event plumes (circles) [*Baker et al.*, 1995], a high-temperature vent field (star) [*Delaney and Embley*, 1993], and earthquake locations obtained from the analysis of tertiary-phase records recorded by the U.S. Navy Sound Surveillance System (dots) [*Dziak et al.*, 1995].

event plumes might form as a result of direct interactions between a seafloor eruption and seawater but subsequently argue that the rise heights and chemistry are incompatible with such a mechanism [*Baker et al.*, 1989]. *Baker et al.* [1987, 1989] also hypothesize that rifting events might release a reservoir of hot fluid, although it is difficult to envision how large volumes of fluid could be trapped in an extensional environment [*Cann and Strens*, 1989]. On the basis of observations in the Troodos ophiolite, *Cann and Strens* [1989] argue that a resistive cap and shell develops around upflow zones because of the precipitation of hydrothermal minerals in regions where hot and cold fluids mix. The resistive cap controls the fluid flux through the system. When the cap is fractured as the result of either a rifting event or by the progressive build up of hydrostatic pressure, fluxes through the whole system increase dramatically, and high fluxes persist until the system reclogs or the heat content is exhausted. *Cathles* [1993] postulates that the fluid fluxes of mid-ocean ridge hydrothermal systems are controlled by the permeability of a very thin but areally extensive flow zone located on the sides of the axial intrusion. He argues that an event plume can result from the collapse of the thermal boundary layer in the flow zone following an increase in permeability due to magma withdrawal, thermal contraction, or a pulse of magmatic volatiles. The thermal energy in the event plume can be equated to the heat content of the flow zone. *Nehlig* [1993, 1994] also suggests that event plumes may be initiated by the release of magmatic fluids trapped in the axial magma chamber. *Lowell and Germanovich* [1995] argue that the emplacement of a dike increases the average permeability in upflow zones by several orders of magnitude. They present a simple model in which event plume formation over a period of ~10 days is driven by the heat content of the dike. However, this timescale is significantly longer than the estimated formation times of the CoAxial event plumes [*Lavelle*, 1995] and a 1-m-wide dike may not contain sufficient heat to generate the Cleft event plumes. Most recently, *Butterfield et al.* [1997], citing recent observations on the CoAxial segment, have revived the idea that event plumes form by direct interactions with a seafloor eruption. They argue that such a model most simply explains the coincidence of event plumes and seafloor eruptions, the heat contents and very short formation times of event plumes, and the presence of a halite coating on the fresh extrusives.

In this paper, I explore an alternative mechanism first proposed by *Wilcock* [1994] whereby event plumes are generated by fluid expansion in a depressurized reaction zone. If the fracturing accompanying a diking event reduces the hydraulic resistance of the upflow zone more than the downflow zone, the pressures throughout the hydrothermal system must decrease. If the fluids at the base of the system lie near the two-phase boundary, this pressure reduction results in considerable fluid expansion which is balanced by a transient increase in upflow fluxes.

A Fluid Expansion Mechanism for Event Plumes

In the following sections, I develop a simple quantitative model for the fluid expansion mechanism. In the first section, I consider steady state models of hydrothermal circulation to estimate the likely pressure gradients prior to a diking event. Second, I estimate the pressure drop that might follow the intrusion of a dike. Diking can change the permeability structure very quickly, but the thermal inertia of the rock matrix will preserve the same pattern of flow. Given an estimate of the new permeability structure, modified quasi-steady state pressure conditions can be determined by matching upflow and downflow fluxes. In the third section, I consider the increase in fluid volume in the reaction zone that must occur as the pressures decrease and the system evolves between the two steady state configurations. Finally, I develop a simple transient model for the ejection of a plume.

Pressure Gradients in Mid-ocean Ridge Hydrothermal Systems

The pressure gradients which drive hydrothermal circulation result from the difference in hydrostatic pressures between columns of hot and cold fluid. At any location in a hydrothermal system, the total pressure gradient is the sum of the local hydrostatic gradient and the gradient driving flow. If the hydraulic resistance of a hydrothermal system is dominated by the discharge zone, then to balance fluxes the pressure gradients driving downflow must be small, and pressures everywhere must approach cold hydrostatic (Figure 3a). Conversely, in recharge-dominated systems the pressures approach hot hydrostatic.

The pressure gradients can be quantified by considering a pipe model (Figure 4) comprising predefined downflow, reaction (heat uptake), and upflow zones connected into a single-pass system. For a steady state system, the mass fluxes in the upflow and downflow zones must balance. Assuming Darcy flow, this condition requires

$$\frac{1}{R_u}\left(\frac{\partial p'}{\partial z}\right)_u = -\frac{1}{R_d}\left(\frac{\partial p'}{\partial z}\right)_d \tag{1}$$

where R is the hydraulic resistance per unit depth of circulation, p' is the component of the pressure responsible for driving fluid flow, z is the vertical coordinate increasing downward, and the subscripts u and d refer to the upflow and downflow zones, respectively. The terms R_u and R_d are defined

$$R_u = \frac{\mu_h}{A_u k_u \rho_h}$$
$$R_d = \frac{\mu_c}{A_d k_d \rho_c} \tag{2}$$

where A is the cross-sectional area, k is the permeability, ρ and μ are the fluid density and viscosity, respectively, and the subscripts h and c refer to properties of hot and cold fluid, respectively. For simplicity, I neglect the pressure drop driving flow through the reaction zone. Continuity at the base of the model requires that the vertical gradient of the total pressure p is the same in the upflow and downflow zones. The pressure gradients driving flow can be written

$$\left(\frac{\partial p'}{\partial z}\right)_u = \frac{\partial p}{\partial z} - \rho_h g \tag{3}$$

$$\left(\frac{\partial p'}{\partial z}\right)_d = \rho_c g - \frac{\partial p}{\partial z} \tag{4}$$

where g is the acceleration of gravity. Substituting (3) and (4) into (1) and solving for the total pressure gradient yields

$$\frac{\partial p}{\partial z} = \left(\rho_h + (\rho_c - \rho_h)\frac{R_u}{R_u + R_d}\right) g \tag{5}$$

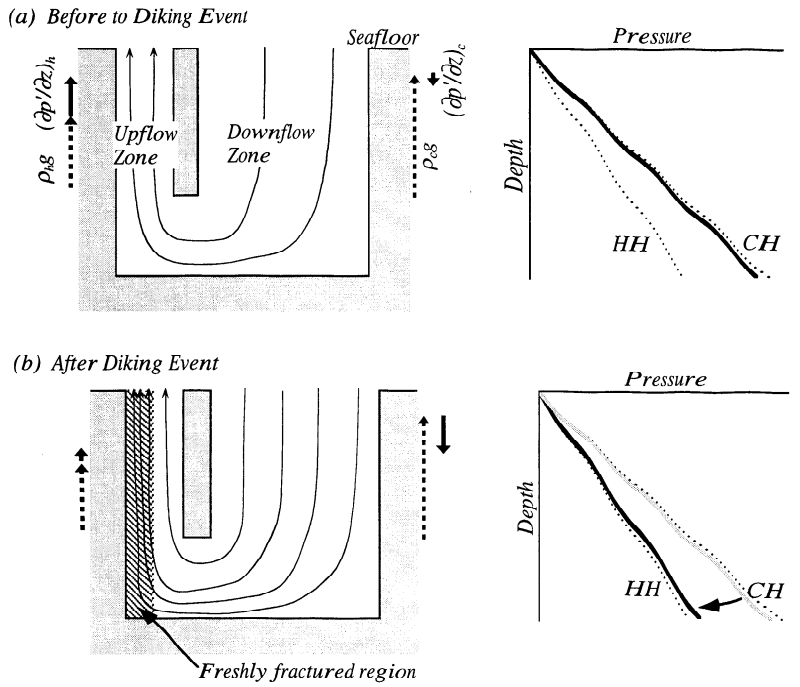

Figure 3. Schematic diagram showing the change in hydrostatic pressure following a diking event. (a) Before the diking event, the hydrostatic resistance of the upflow zone exceeds that of the downflow zone. The total pressure gradient throughout the system, which is the sum of the pressure gradients driving flow (solid vectors) and the hydrostatic pressure gradients (dashed vectors), is much closer to cold hydrostatic (CH) than hot hydrostatic (HH). (b) After a dike-induced decrease in the hydraulic resistance of the upflow zone, the total pressure must move toward hot hydrostatic to balance fluxes. This pressure reduction will be accompanied by the expansion of fluids in the reaction zone, a process which results in a temporary imbalance of fluxes and the expulsion of a transient plume.

The relative values of R_d and R_u are not constrained by pipe models because the cross-sectional area and permeability of the pipe is defined a priori, but some insight into this matter can be obtained from simple solutions for cellular convection.

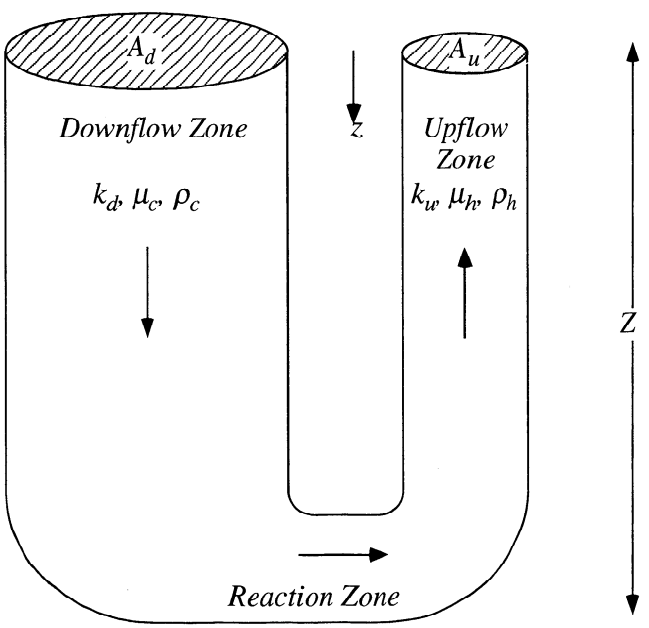

Figure 4. Configuration of the pipe flow model used to quantify the pressure gradients in mid-ocean ridge hydrothermal systems.

Figure 5 shows the configuration of steady convection in an uncapped porous box heated from below at Rayleigh numbers, Ra = 100 and Ra = 1000. The Rayleigh number is a dimensionless number which determines the vigor of convection and is defined

$$Ra = \frac{\alpha g \rho^2 c_p k Z \Delta T}{\mu \lambda} \tag{6}$$

where α is the coefficient of thermal expansion for the fluid, c_p and λ are the heat capacity and thermal conductivity of the saturated porous matrix, respectively, and ΔT is the vertical temperature drop across the convecting layer which has thickness Z. The solutions have been obtained with the Boussinesq approximation (i.e., linear variations in density are considered only in the buoyancy term), and the permeability and viscosity are constant. The solutions show strong similarities to the pipe model; the circulation is single pass, and the flow is nearly vertical within well-developed upflow and downflow zones. At Ra = 100, the widths of upflow and downflow are approximately equal which corresponds to R_u/R_d = 1 in the pipe model (note that because the Boussinesq approximation has been used for the cellular convection calculations, it is appropriate to use $\rho_c = \rho_h$ in (2)). Equation (5) predicts a pressure gradient midway between hot and cold hydrostatic which is consistent with the average pressure gradient observed in the convection solution (Figure 5a). As the vigor of convection increases, the thermal fluxes increase and the thickness of the basal thermal boundary layer decreases. Since the boundary layer feeds into the upflow zone, the width of upflow also decreases. At Ra = 1000, $R_u/R_d \approx 2$, and the pressure gradients are consequently higher.

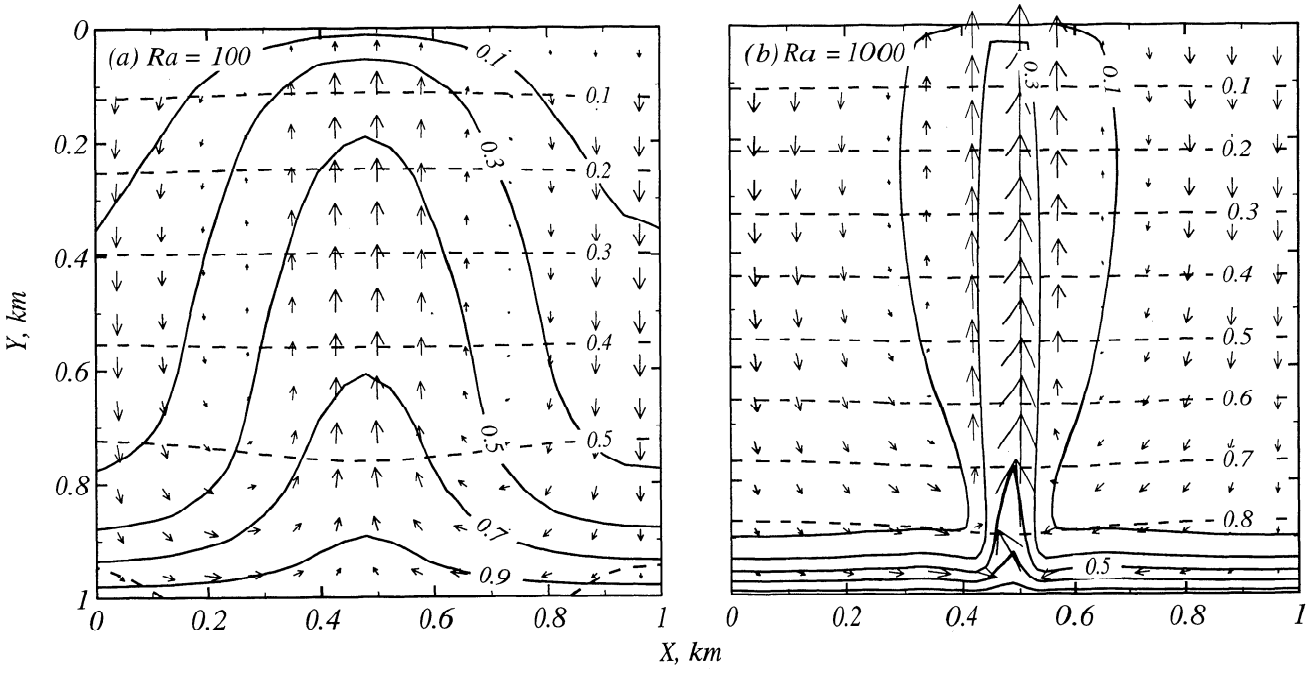

Figure 5. Examples of nondimensionalized solutions for porous convection in an uncapped square box heated from below at Rayleigh numbers of (a) 100 and (b) 1000. For purposes of comparison, the minimum Rayleigh number required for convection is ~30, while the Rayleigh number for systems feeding large black-smoker vent fields may reach about 10^4-10^5 [*Lister*, 1983; *Wilcock and McNabb*, 1995]. The solutions were obtained using a finite volume algorithm [*Patankar*, 1980] and a uniform 24 by 24 grid. The viscosity and coefficient of thermal expansion of the fluid and the permeability of the medium are assumed constant. The dimensionless temperature is held at 0 and 1 at the top and bottom boundaries, respectively, and the pressure on the top boundary is 0. The bottom boundary is impermeable, and the side boundaries enforce periodicity. Vectors show the direction and relative speed of fluid flow; for display purposes, vectors in Figure 5a are scaled by a factor of 5 relative to Figure 5b. Contours show the dimensionless temperature (solid) and pressure (dashed). The nondimensional hydrostatic pressures gradient is 0 and 1 in columns at temperatures of 1 and 0, respectively. For Ra = 100, the mean temperatures of upwelling and downwelling fluids are 0.6 and 0.2, respectively. The average pressure gradient in the system is 0.6 which lies midway between the appropriate hot (0.4) and cold (0.8) hydrostatic gradients. For Ra = 1000, the temperature in the core of the upwelling column is 0.3 which is equivalent to a hydrostatic pressure gradient of 0.7. The temperature of downwelling is close to 0. The vertical pressure gradient throughout the model is about 0.9, so the pressure gradient driving upflow is about twice that driving downflow.

The Rayleigh numbers for some black-smoker systems probably reach 10^4-10^5 [*Lister*, 1983; *Wilcock and McNabb*, 1995]. The steady solutions suggest that R_u/R_d may be large for such systems. Some caution is warranted when extrapolating results derived from steady convection models obtained with the Boussinesq approximation and constant fluid properties to real hydrothermal systems. The flow in the widest cracks is almost certainly turbulent and will not obey Darcy's law. At sufficiently high Rayleigh numbers, convection will be unsteady, and the characteristics of such flow have not been studied in detail for open-top systems. The viscosity of water is strongly temperature dependent, the buoyancy of hydrothermal fluids varies nonlinearly with temperature, and two-phase flow can be expected near the base of many systems. However, there is other evidence that the pressures in vigorous systems approach cold hydrostatic. Relatively shallow measurements of borehole pressures in vigorous liquid-dominated systems on land, such as Taupo geothermal region, New Zealand, reveal pressure gradients approximately midway between hot and cold hydrostatic [*Grant et al.*, 1982]. Observations of these systems suggest that the cross-sectional area of the upflow region decreases with depth [*Elder*, 1965, 1981]. Pipe models which match heat and chemical fluxes require deep pressure gradients near cold hydrostatic [*Elder*, 1965, 1981]. The small area of high-temperature vent fields along mid-ocean ridges suggests that these systems are also discharge dominated [*Lowell and Germanovich*, 1994; *Wilcock and McNabb*, 1995].

Pressure Drop Following a Dike Intrusion

The intrusion of a dike is accompanied by considerable faulting and fracturing as evidenced by the extensive seismic swarms observed on Krafla volcano in Iceland [*Brandsdóttir and Einarsson*, 1979; *Einarsson and Brandsdóttir*, 1980], Kilauea and Mauna Loa volcanoes in Hawaii [*Klein et al.*, 1987], and the CoAxial segment [*Dziak et al.*, 1995]. Swarm earthquakes have local magnitudes up to 3 and are confined to a narrow zone, which even with hypocentral location errors, may extend as little as 1 km to either side of the intrusion. Where dikes do not reach the surface, shallow extension is accommodated by normal faulting above and in front of the laterally propagating dike [*Rubin*, 1992]. Field observations from several locations show that diking can be accompanied by the formation of dike parallel joints in a region extending 10-100

m from the dike [*Andrews and Emeleus*, 1975; *Delaney et al.*, 1986; *Rogers and Bird*, 1987]. *Rubin* [1993] presents a mechanical model for the tensile fracturing accompanying dike propagation which predicts both tensile fracture and strike-slip failure on dike-parallel planes extending several meters to either side of the dike. Boiling of heated hydrothermal fluids adjacent to the rock may also contribute to crack formation [*Germanovich and Lowell*, 1995].

Observations from volcanically active mid-ocean ridge segments show that hydrothermal vent sites coincide very closely with the axis of accretion [e.g., *Fornari and Embley*, 1995]. Faulting and fracturing in a narrow zone surrounding a dike is likely to produce a large increase in the permeability of the upflow zone [*Lowell and Germanovich*, 1995]. The distribution of downflow is poorly known, but unless circulation is recharge-dominated, downflow zones must extend over a much larger area because the viscosity of cold seawater is over an order of magnitude higher than hot hydrothermal fluid. For most geologically plausible patterns of circulation, dike-induced permeability will have a much smaller effect on the overall hydraulic resistance of the downflow zone. Indeed, the hydraulic resistance to downflow may be unchanged if recharge is confined to inward facing normal faults on the ridge flanks.

If the relative hydraulic resistance of the upflow zone decreases, then to balance mass fluxes either the horizontal extent of upflow must decrease or the pressure gradients driving flow must change. The configuration of flow can change only very slowly because the rock matrix provides considerable thermal inertia. In the short term, the pressure gradients driving upflow must decrease and those driving downflow must increase, and the total pressure gradient must decrease toward hot hydrostatic (Figure 3b). If the initial configuration is recharge-dominated and the final configuration is discharge-dominated, the pressure drop at the base of a system is about $3Z$ MPa, where Z is the depth of circulation below the seafloor in kilometers (Figure 3b). The pressures cannot drop instantaneously following a diking event because hydrothermal fluids are compressible. Initially, the pressures will be unchanged, upflow fluxes will greatly exceed downflow fluxes, and the difference will be balanced by fluid expansion. As the fluids expand, the pressure will decline progressively until the mass fluxes through the system are balanced.

Given an estimate of the ratio R_u/R_d before and after a diking event, (5) can be used to infer the change in the total pressure gradient. For an initial $R_u/R_d \sim 1$, a relatively modest decrease in upflow resistance can decrease pressures gradients substantially. Taking $R_u = R_d$ and fluid densities given in Table 1, the initial pressure gradient is 8.5 MPa km^{-1}. For final ratios R_u/R_d of 0.5 and 0.1, the pressure gradients decrease to 7.9 MPa km^{-1} and 7.0 MPa km^{-1}, respectively. When the initial $R_u/R_d \gg 1$, as might be expected in vigorous discharge-dominated systems, the reduction in pressure is always small for modest decreases in R_u. However, the fluxes required to form event plumes exceed those of a sizable high-temperature vent field by up to 3 orders of magnitude. This observation requires that R_u decrease by a similar factor if the plumes are to form from hydrothermal fluids deep within the system. If the dike only increases permeability in a narrow region and downflow extends over a relatively large area, the change in R_d will be much smaller. For example, assuming an initial $R_u/R_d = 10$, a uniform permeability, and fluid properties from Table 1, (2) gives $A_d \approx 100A_u$. If the permeability increases by a very large factor in a volume which includes all the upflow zone and one tenth the downflow zone, R_u/R_d decreases to 1 and the pressure gradients will drop from 10.0 MPa km^{-1} to 8.5 MPa km^{-1}. If the diking event does not significantly affect the downflow zone, R_u/R_d decreases to 0.1 and the pressure gradients will drop to 7.0 MPa km^{-1}. Cumulatively, these considerations suggest that the pressure drop in the reaction zone following a diking event will probably be at least $1.5Z$ MPa and may reach $3Z$ MPa in vigorous systems.

Table 1. Fluid and Rock Properties Used for the Calculations

Symbol	Meaning	Value
ρ_h	Density of hot (350°C) hydrothermal fluid	670 kg m^{-3}
ρ_c	Density of cold (0°C) seawater	1030 kg m^{-3}
μ_h	Viscosity of hot hydrothermal fluid	7 x 10^{-5} Pa s
μ_h	Viscosity of cold seawater	2 x 10^{-3} Pa s
$c_{p,r}$	Specific heat capacity of basaltic rock	1 x 10^{3} J kg^{-1}
ρ_r	Density of basaltic rock	2800 kg m^{-3}
T_{mp}	Temperature of fluid released into the megaplume	350°C
c_p	Mean specific heat capacity of hydrothermal fluids (0° to 350°C)	4500 J kg^{-1} °C^{-1}

Fluid properties are based on *Grigull et al.* [1984] and *Anderko and Pitzer* [1993].

Plume Volumes

The compressibilities of cold seawater (~5 x 10^{-4} MPa^{-1}) [*Grigull et al.*, 1984] and hot hydrothermal fluid at 350°C (~5 x 10^{-3} MPa^{-1}) [*Anderko and Pitzer*, 1993] are sufficient only for increases in fluid volume of ~0.1% and ~1% in the downflow and upflow zones, respectively. However, there is extensive evidence to suggest that the fluids in reaction zones at the base of systems may be very compressible. The salinity of hydrothermal fluids can vary from a small fraction to about twice that of seawater, an observation that is best explained by two-phase separation followed by partial remixing and dilution with seawater [*Delaney et al.*, 1987; *Von Damm*, 1988; *Cowan and Cann*, 1988; *Bischoff and Rosenbauer*, 1989]. Salinity variations in hydrothermally derived fluid inclusions from high-level plutonic intrusions are remarkably similar to those observed in vent fluids and require two-phase separation at temperatures of 400°-500°C [*Kelley and Robinson*, 1990; *Nehlig*, 1991; *Kelley et al.*, 1993; *Kelley and Malpus*, 1996]. Mineral solubility experiments [*Seyfried*, 1987; *Berndt et al.*, 1989] and theoretical phase relations [*Seyfried et al.*, 1991] suggest that reaction zone temperatures of at least 375°-410°C and pressures of 40 MPa are required to reproduce the chemistry of hot spring fluids. Alteration assemblages from near the dike-gabbro transition in both ophiolites and mid-ocean ridges require temperatures in the range 400°-500°C [*Gillis and Robinson*, 1990; *Gillis et al.*, 1993; *Nehlig*, 1994; *Gillis*, 1994]. At these temperatures and hydrostatic pressures corresponding to depths of 1-3 km, hydrothermal fluids lie near the supercritical portion of the two-phase curve for seawater where compressibilities are high in both the one- and two-phase region (Figure 6).

The change in fluid volume accompanying a pressure drop is dependent on the pressure-temperature path followed by the fluid. If the fluid depressurizes in isolation, it will follow an adiabatic path [*Bischoff and Pitzer*, 1985; *Cann et al.*, 1985]. For the sudden pressure drops predicted by this model, the appropriate path may be isoenthalpic rather than isoentropic, al-

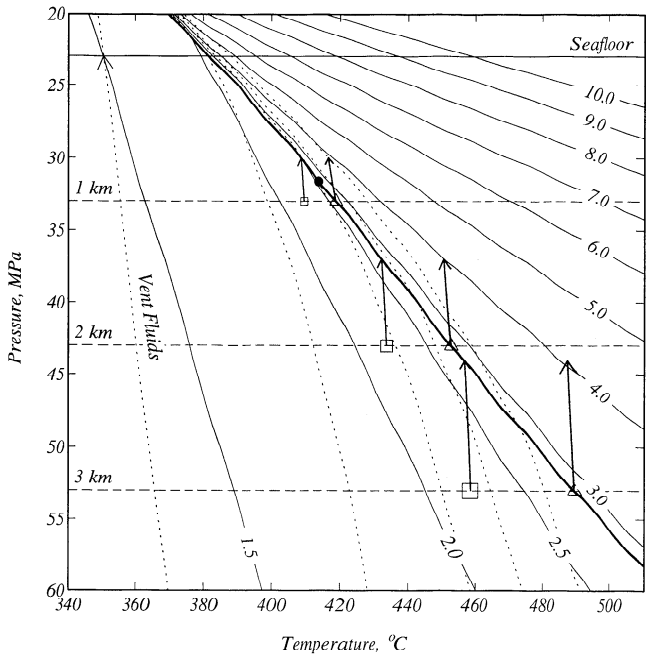

Figure 6. Phase diagram for seawater (3.2 weight percent NaCl solution) [*Anderko and Pitzer,* 1993] showing the two-phase curve (bold), the critical point (circle), labeled contours of specific volume (1000 × m^3 kg^{-1}) (solid), and isenthalps (dashed). The isenthalp labeled "Vent Fluids" shows an adiabatic path for fluids venting at 350°C. Solid vectors show examples of decompression curves for a pressure drop of 3.0 MPa km^{-1} calculated by contouring equation (7) with ϕ = 0.05 and ε = 0.5. The fractional changes in volume along these paths are presented in Figure 7. Squares and triangles at the start of these paths and arrows at the end facilitate the identification of the equivalent paths in Figure 7. The shaded region shows the likely conditions in the reaction zones above mid-ocean ridge magma chambers inferred from other studies (see text). The pressure at the seafloor is based on a water depth of 2250 m which is appropriate for the Juan de Fuca Ridge, and the depths below seafloor are calculated for a hydrostatic pressure gradient of 10.0 MPa km^{-1}.

though for seawater the distinction is not important because the paths are similar. In real hydrothermal systems, the fluid cannot expand entirely in isolation since it is in contact with the rock matrix. The volumetric heat capacity of basalt and water are approximately equal, so for reasonable porosities, the heat content of the system is dominated by the rock. For a thermal diffusivity of 10^{-6} m^2 s^{-1}, event plume formation times of a few hours to a few days yield a thermal diffusion length scale of 0.1-0.5 m. Observations in ophiolites [e.g., *Nehlig,* 1994] and conceptual models of the fracture system feeding into hydrothermal upflow zones [*Goldfarb and Delaney,* 1988] suggest that this length scale is similar to the spacing of cracks in the reaction zone. The fluids must expand in near thermal equilibrium with much of the rock along paths that are more nearly isothermal. If the fluid expands in place, the paths can be approximated by

$$H(T,p)+\varepsilon\frac{1-\phi}{\phi}\frac{\rho_r c_{p,r} T}{\rho_0}=C \qquad (7)$$

where H is the enthalpy of the hydrothermal fluid and is a function of temperature T and pressure p, ε is the fraction of the rock in thermal equilibrium with the fluid, ϕ is the porosity, ρ_r and $c_{p,r}$ are the density and specific heat capacity of the rock, respectively, ρ_0 is the density of the hydrothermal fluid before decompression, and C is a constant.

The solid vectors in Figure 6 show paths obtained from (7) assuming a porosity of 5%, ε = 0.5, and physical properties given in Table 1. The paths are appropriate for reaction zone depths of 1-3 km and a pressure drop of 3 MPa km^{-1} and are chosen to either end or start on the two-phase curve. Figure 7 shows the fractional volume changes as a function of the pres-

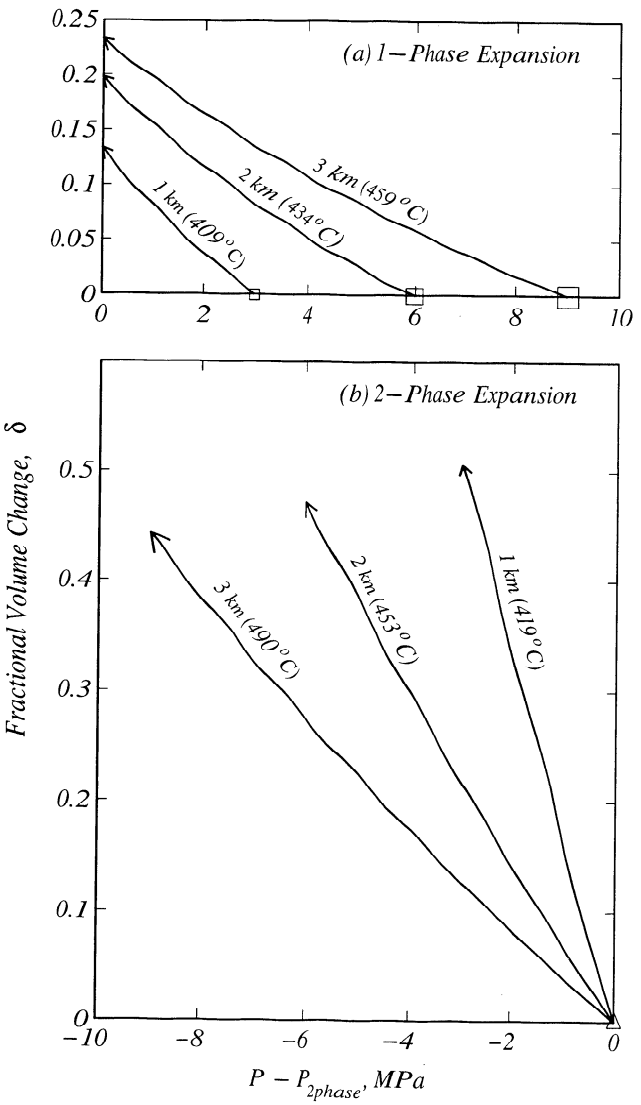

Figure 7. Fractional increase in seawater volume δ observed for conditions near the two-phase curve when the pressure decreases by 3 MPa km^{-1} along pressure-temperature paths derived from equation (7). The pressure-temperature paths are shown in Figure 6. The starting pressures are appropriate for depths of 1, 2, and 3 km below the seafloor (based on a seafloor depth of 2250 m and an initial hydrostatic pressure gradient of 10 MPa km^{-1}). The starting temperatures (labeled) are chosen so the paths either (a) end or (b) start on the two-phase curve. Pressures are plotted relative to the pressure at the intersection of the fluid path and the two-phase curve. Squares and triangles at the start of these paths and arrows at the end facilitate the identification of the equivalent paths in Figure 6.

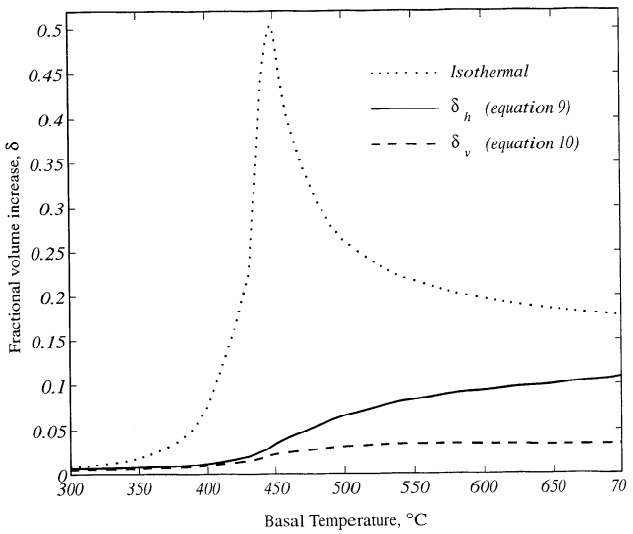

Figure 8. Mean fractional increase in seawater volume as a function of the maximum temperature for a pressure drop of 3 MPa km^{-1} in a 200-m-thick reaction zone at a depth of 2 km below the seafloor (assuming a seafloor depth of 2250 m and an initial hydrostatic pressure gradient of 10 MPa km^{-1}). Curves are plotted for an isothermal reaction zone (dotted) and a reaction zone in which the temperature increases linearly with depth from 0°C to the maximum value. For this latter configuration, the volume increase is shown assuming the fluids expand either horizontally (solid) or vertically (dashed).

sure drop along these paths. For a 3-MPa km^{-1} pressure reduction, the volume increases by 10-25% in the one-phase region and about 50% in the two-phase region. Figure 8 shows the average volume increase as a function of temperature for a 3-MPa km^{-1} pressure reduction at 1.8-2 km depth below the seafloor (the ocean depth is 2250 m). As the reaction zone temperature increases from 300°C to 450°C, the amount of expansion increases rapidly from 1% to over 50% and then decreases to 15-20% at temperatures above 550°C.

It is clear from Figure 8 that the size of the plume generated by the fluid expansion mechanism is critically dependent on the temperature conditions. As I noted above, there is extensive evidence that the temperatures in the reaction zone reach values well above observed venting temperatures, but the size and structure of the high-temperature region is not known. Observations for continental systems suggest that the reaction zone is generally overlain by a relatively impermeable region [*White*, 1973]. As a result, the reaction zone is nearly isothermal with high-temperature gradients in the overlying cap rock. *Richardson et al.* [1987] estimate volumes of several cubic kilometers for the reaction zones beneath the massive sulfide deposits of the Troodos ophiolite. If a reaction zone of similar size were filled with fluids near the two-phase curve, the decrease in pressure following the emplacement of a dike might be sufficient to generate a very large plume. For example, the 1986 Cleft event plume (~0.1 km^3) could result from a 50% increase in fluid volume in a 4 km^3 reaction zone with a porosity of 5%, while the CoAxial event plumes (~0.005-0.01 km^3) could result from a 20% volume increase within a 1 km^3 reaction zone with a porosity of 2.5-5%. However, if the reaction zone is filled with fluids at 350°-400°C, which rise adiabatically to vent sites with little conductive cooling, the resulting plumes would be considerably smaller. Moreover, the geological observations do not require that the entire fossilized reaction zone was active at one time. Even if the reaction zone lies near the two-phase boundary, fluid expansion will generate relatively small plumes if it is confined to a thin thermal boundary layer which migrates downward behind a cracking front [*Lister*, 1974, 1983]. The porosity of the reaction zone may be only ≤1% if porosity is created primarily by horizontal thermal contraction [*Lister*, 1974, 1983].

There are at least reasons to question whether the reaction zones of mid-ocean ridge systems are isothermal. It is difficult to reconcile the maximum inferred reaction zone temperatures of at least 400°-500°C with the observed maximum venting temperatures of 320°-380°C. Adiabatic gradients for venting fluids are only a few degrees per kilometer (Figure 6), and upwelling fluids cool conductively by no more than a few tens of degrees [*Berndt et al.*, 1989; *Seyfried et al.*, 1991]. This apparent temperature discrepancy can be eliminated if the vent fluids are a mixture of fluids circulating at different depths through a reaction zone with a vertical temperature gradient. It is unclear whether the relatively low permeability cap which is associated with isothermal reaction zones in continental systems can form in the ridge environment. When downwelling seawater heats up to about 150°C, anhydrite precipitation [*Seyfried*, 1987] will tend to seal cracks above the reaction zone and quartz precipitation will act to clog the upflow zone [*Lowell et al.*, 1993]. However, the extensional tectonics of the ridge environment will act to keep cracks open at all depths. In continental systems, chemical processes may increase reaction zone permeability; there is clearly a net transport of minerals out of the system because downwelling meteoric water reemerges as the mineral-laden waters of hot springs. In oceanic systems, the picture is more complex. The ionic strength is primarily controlled by the chlorinity which is conserved within the fluid as a whole. While silica is transported out of the crust, there is a net transport of metal ions into the crust, not only as a result of anhydrite precipitation above the reaction zone but also because the *p*H decreases within the reaction zone [*Seyfried*, 1987].

An alternative estimate of the volumes of expansion plumes can be obtained from a simple model based on the cellular convection solutions (Figure 5). The thermal boundary layer is equated to the reaction zone and is assumed to have a uniform thickness h. The temperature T varies linearly between a prescribed basal temperature T_{max} and 0°C at the top of the boundary layer

$$T(z) = T_{max}\frac{z - Z + h}{h} \tag{8}$$

In the limit of no convection, $h = Z$ yields a conductive temperature profile, while for vigorous convection the high heat flux requires $h << Z$. Upon decompression, the fluids in the thermal boundary layer may expand either horizontally or vertically upward. By making the simplifying approximation that the heat content of the rock matrix maintains the initial temperature, the mean fractional change in fluid volume δ within the reaction zone can be approximated

$$\delta_h = \frac{1}{h}\int_{Z-h}^{Z}\left[\frac{\rho\left(T(z), p_{sf} + \rho_0 g z\right)}{\rho\left(T(z), p_{sf} + \rho_1 g z\right)} - 1\right]dz \tag{9}$$

for horizontal expansion and

$$\delta_v = \frac{1}{h}\frac{\int_{Z-h}^{Z}\left[\rho\left(T(z), p_{sf}+\rho_0 gz\right)-\rho\left(T(z), p_{sf}+\rho_1 gz\right)\right]}{\rho\left(T_{mp}, p_{sf}\right)}dz \quad (10)$$

for vertical expansion, where p_{sf} is the pressure at the seafloor, T_p is the temperature of fluids discharged into the plume, and $\rho_0 g$ and $\rho_1 g$ are the pressure gradients before and after decompression, respectively.

Figure 8 also shows δ_h and δ_v as a function of basal temperature for a 200-m-thick boundary layer, circulation to a depth of 2 km, and a pressure drop from 10 to 7 MPa km^{-1}. For a reasonable range of parameters, δ_h and δ_v are essentially independent of the reaction zone thickness and linearly proportional to the pressure drop. For vertical expansion, the fluids cool because they expand upward into colder rock, and the resulting volume increase is about half that for horizontal expansion. In a real system, there must be a component of both vertical and horizontal expansion. To eject a plume, fluids must be expelled upward, but the fluid volumes increase on average by only a small fraction, and so most of the fluid remains in the thermal boundary layer. If the cross-sectional area of upflow zone is relatively small, most of the thermal boundary layer underlies downflow, and here the fluids must expand horizontally. The volume increases obtained for the linear boundary layer model are much smaller than those for an isothermal reaction zone. For a 4-km^3 reaction zone with 5% porosity and a basal temperature of 500°C, the plume volumes estimated from (9) and (10) are ~0.01 km^3. This is about a tenth of the maximum plume size estimated for an isothermal reaction zone of the same dimensions. This calculation is compatible with the observed volume of the CoAxial plumes, but the larger volume of the Cleft plumes can only be matched if volume, porosity, and basal temperature are relatively large.

The plume volume estimates derived from the isothermal and linear boundary layer models are most sensibly viewed as upper and lower bounds. Numerical studies show that at high Rayleigh numbers unsteady patterns of flow develop because secondary convective instabilities form within the thermal boundary layer [e.g., *Caltagirone and Fabrie*, 1989]. These instabilities would tend to even out the temperature leading to a mean temperature structure intermediate between the linear boundary layer and isothermal models.

McNabb and Fenner [1985] and *Bischoff and Rosenbauer* [1989] present an alternative model for the structure of mid-ocean ridge hydrothermal systems in which two-phase separation at the base of the system results in double diffusive convection with a single-pass seawater cell underlain by a convecting brine layer. The salinity and temperature in the brine layer are dependent upon the pressure but increase with depth to maximum values of ~50 wt % NaCl and 600°-700°C. The brine lies close to its boiling point throughout its cycle. This model is compatible with the observations of two-phase separation in many systems and may provide an explanation for venting temperatures [*Bischoff and Rosenbauer*, 1989]. Temperatures derived from amphibole veins [*Nehlig and Juteau*, 1988; *Gillis et al.*, 1993; *Nehlig*, 1994] and oxygen isotopes [*Stakes*, 1991] suggest that fluids circulate through gabbros at >600°C. A brine rich layer near the boiling point could contribute significantly to the volume of plumes. For example, a pressure drop of 1.5-3 MPa km^{-1} in a 50 wt % NaCl brine on the boiling curve at 4 km depth results in a volume increase of 30-60%, and this result is not strongly dependent upon the salinity. Boiling within a 300-m-thick brine layer of 5% porosity could match the volumes of the Cleft event plume if the layer extended over ~10 km^2.

The fracturing accompanying a diking event may also open up pathways to fluids under lithostatic pressures. Mid-ocean ridge hydrothermal circulation is clearly episodic, and while hydrothermal circulation will certainly cease when the heat source is exhausted, it will also stop if mineral precipitation can clog the flow paths. Any fluids trapped below a sealed horizon will evolve toward lithostatic pressures in response to matrix deformation and thermal expansion accompanying conductive reheating. The volume increases following a change from lithostatic to hydrostatic pressure are strongly dependent on the temperature of the fluid. At midcrustal hydrostatic pressures, seawater lies within the two-phase region at temperatures in excess of ~500°C (Figure 6). At 500°C and 3 km depth, the specific volume of seawater will increase about 100% from ~1.8 x 10^{-3} m^3 kg^{-1} to >3.0 x10^{-3} m^3 kg^{-1} (Figure 6) as the pressure changes from lithostatic to hydrostatic, while at 600°-700°C the volume increases several hundred percent. Similar volume increases would occur in a NaCl-rich brine. The release of a relatively small volume of high-temperature fluids at lithostatic pressures would contribute significantly to the volume of plumes.

Plume Formation Times

In order to model the formation of an event plume, I consider a simple model (Figure 9) comprising expansion in a reaction zone at depth Z with a fluid volume V_R. The event plume is driven by an excess pressure p' through a channel of width d, length l, and permeability k. Because the plume forms quickly and the pressures can never exceed cold hydrostatic and drive cold fluids upward, I treat the downflow region as a static region surrounding the reaction zone. The model is analogous to lifting the valve off a pressure cooker. Using Darcy's law, the heat flux can be written

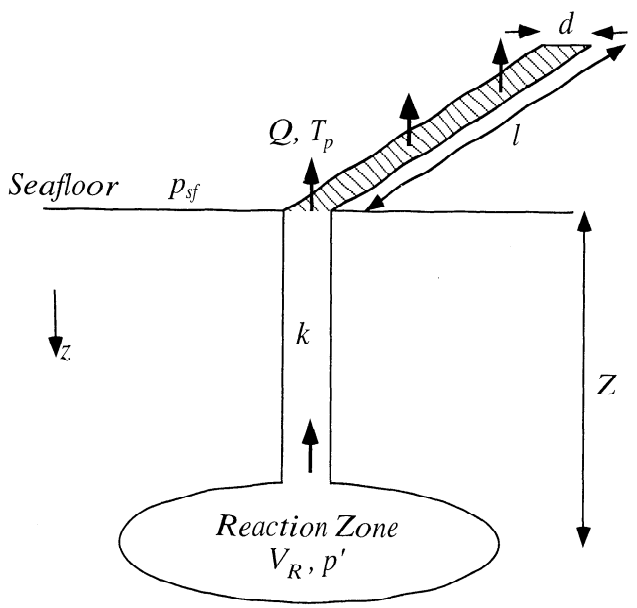

Figure 9. Configuration used to model the formation of transient plumes.

$$Q = \rho_h c_p T_p dl \frac{k}{\mu} \frac{p'}{Z} \quad (11)$$

where c_p is the heat capacity of hydrothermal fluids averaged between 0°C and T_p. The maximum plume rise heights above the seafloor place strong constraints on the initial heat flux Q_0. Assuming emission from a line source, *Baker et al.* [1989] and *Lavelle* [1995] estimate Q_0/l to be 3.5 x 10^8 W m^{-1} and 1.7 x 10^8 W m^{-1} for the 1986 Cleft and CoAxial event plumes, respectively. Assuming the initial excess pressure p_0 is given by p'_0/Z = 1.5-3 MPa km^{-1} and values for fluid properties presented in Table 1, these heat fluxes yield a product kd = 4 x 10^{-9} to 2 x 10^{-8} m^3. For reasonable values of d ranging from 10-100 m, the required permeabilities are ~10^{-10} to 10^{-9} m^2.

Unless the flow occurs in very thin cracks, the flow will be turbulent [*Cann and Strens*, 1989; *Lowell and Germanovich*, 1995]. The heat flux carried by turbulent flow through n dike-parallel rough cracks of width w can be written [*Schlichting*, 1979; *Middleton and Southard*, 1984]

$$Q = n\rho_h c_p T_{mp} lw \sqrt{\frac{4w}{\rho f} \frac{p'}{Z}} \quad (12)$$

where f is the friction factor which depends on the roughness of the crack walls. For $f \approx 0.05$ and excess pressure gradients of 1.5-3 MPa km^{-1}, the required flow rates can be supported by turbulent flow through a single 5-cm-wide crack or about ten 1-cm-wide cracks. The amount of extension accommodated by fractures during a diking event is unknown, but the total width of cracks required is only a small fraction of the typical width of a dike.

Assuming a constant compressibility β in the reaction zone and neglecting compressibility in the upflow zone and the change in effective k with p' that results from turbulent flow, the decline in p' with time t can be approximated

$$p' = p'_0 \exp\left(-\frac{t}{\gamma}\right) \quad (13)$$

where the exponential decay time γ is the characteristic formation time of the event plume and is given by

$$\gamma = \frac{\mu_h Z V_R \beta}{kdl} \quad (14)$$

Substituting (13) into (11) and integrating over time, the cumulative energy release is

$$E = \int_0^t Q dt' = E_\infty \left[1 - \exp(-\gamma t)\right] \quad (15)$$

where

$$E_\infty = \rho_h c_p \Delta T V_R \beta p'_0 \quad (16)$$

is the total energy released into the plume.

Estimates of the characteristic formation time γ from the event plumes observations do not provide an independent estimate of kd since the estimates of formation times are themselves derived from the heat fluxes. However, the model can be usefully compared with the vertical structure of event plumes. Dimensional analysis shows that the rise height H of a buoyant plume released into a uniformly stratified fluid is only weakly dependent on the heat flux. For a point source [*Turner*, 1973], the relationship is

$$H \propto Q^{1/4} \quad (17)$$

while for a line source [*Lavelle*, 1995], it is

$$H \propto \left(\frac{Q}{l}\right)^{1/3} \quad (18)$$

Although event plumes are best modeled by line sources, the maximum rise height may be similar to the source length [*Baker et al.*, 1989; *Lavelle*, 1995] in which case the power law relationship between H and Q is presumably intermediate between (17) and (18). These relationships suggest that about 90% of the plume energy will be injected above half the maximum plume rise height. If the flow within the upflow zone is turbulent, this percentage will increase because the heat flux in (12) is only proportional to the square root of p'. These predictions seem generally compatible with observations of the youngest event plumes. The 1986 Cleft event plume extended from 300 to 1000 m above the seafloor with the largest temperature anomalies near the top of the plume [*Baker et al.*, 1989]. Event plume 93A on the CoAxial extended from 400 to 900 m above the seafloor with the largest temperature anomaly at about 800 m [*Baker et al.*, 1995].

The simplified model presented above ignores the flow resistance of the reaction zone itself. Rather than being concentrated beneath the upflow zone, the reaction zone fluids will probably be distributed in a thin thermal boundary layer with horizontal dimensions similar to the height of the upflow zone. The expanding fluids may have to flow a significant horizontal distance before entering the upflow zone. To account very approximately for this effect, the term kd in (14) should be replaced by the sum of kd and the product of the height and horizontal permeability of the reaction zone.

Discussion and Conclusions

I have presented a model for the formation of transient hydrothermal plumes above mid-ocean ridges resulting from fluid expansion within a depressurized reaction zone. The model differs from earlier models [*Cann and Strens*, 1989; *Cathles* 1993; *Lowell and Germanovich*, 1993] in two important ways. First, the resulting plume is composed entirely of mature hydrothermal fluids. Second, the model does not require high permeabilities in the downflow zone since the high fluxes producing the event plume occur only in the upflow zone.

The volume of the plume generated by the fluid expansion mechanism depends not only on the size and porosity of the reaction zone but also on the temperature structure. Large plumes are possible only if there is a substantial volume of hydrothermal fluid at temperatures near the two-phase boundary. For instance, if the temperature of an isothermal reaction zone 2 km beneath the seafloor is 450°C, the increase in fluid volume following a pressure drop of 3 MPa km^{-1} is 50% (Figure 8). At such conditions, the Cleft and CoAxial event plumes can be generated from reaction zones with fluid volumes of 0.01-0.02 km^3 and 0.1-0.2 km^3, respectively. If the temperature is reduced to 350°C, the volume increase is <2%. At these lower temperatures, the boundary layer collapse mechanism of *Cathles* [1993] provides a more viable mechanism to generate large plumes. If the temperatures within the reaction zone are not isothermal but increase linearly with depth from 0°C to temperatures near the two-phase boundary, the change in fluid volume is <10%. The presence of either a high-temperature brine layer or a significant volume of hydrothermal fluids trapped under lithostatic pressures could in-

crease the volume of the plume significantly. Since the size, porosity, and thermal structure of the hydrothermal reaction zones beneath mid-ocean ridge ridges are all poorly known, it is impossible to state categorically whether or not the fluid expansion mechanism can generate a plume of sufficient size.

Like earlier models [*Cann and Strens*, 1989; *Cathles* 1993; *Lowell and Germanovich*, 1993], the fluid expansion mechanism requires very high permeabilities in the upflow zone in order to support the fluxes required for event plume formation. If upflow occurs in a 10- to 100-m-wide zone, the effective permeability must be $\sim 10^{-10}$-10^{-9} m^2 which is equivalent to turbulent flow through about ten 1-cm-wide cracks. *Lowell and Germanovich* [1995] argue that fracturing during dike emplacement will enhance the permeability adjacent to a dike, but it has not been demonstrated that this mechanism can generate sufficient permeability. The fluid expansion mechanism also requires very high permeabilities in the reaction zone since the expanding fluids must move rapidly from this region into the plume. Such high permeabilities suggest that the reaction zone must be well mixed convectively and relatively isothermal. This leads to the conclusion that the larger plume volume estimates obtained for an isothermal reaction zone are more self-consistent than those obtained assuming a linear vertical temperature gradient.

Although previous researchers discounted such a mechanism, *Butterfield et al.* [1997] argue that the CoAxial event plumes formed by direct interactions between surface extrusives and seawater. There is no evidence for hydrothermal discharge at the flow site prior to the eruption, so it is difficult to invoke the presence of a large reservoir of high-temperature hydrothermal fluid. Two of the event plumes were found above the extrusion, while the position of the third was consistent with southward advection away from this site. The total heat content of the known event plumes was about two thirds that of the extrusion. Halite coatings and sulfide minerals precipitated on lava samples recovered by submersible are indicative of an initial period of high-temperature water-rock interactions [*Butterfield et al.*, 1997].

The ^{3}He/heat ratios have been cited as evidence that event plumes are formed from mature hydrothermal fluids. The ^{3}He/heat ratios are low in event plumes [*Lupton et al.*, 1989, 1995], while chronic plumes along volcanically active ridges such as the Cleft [*Lupton et al.*, 1989; *Baker and Lupton*, 1990; *Massoth et al.*, 1994], CoAxial [*Lupton et al.*, 1995], and EPR near 9°50'N (M. D. Lilley and J. E. Lupton, personal communication, 1996) are characterized by ^{3}He/heat ratios that are initially high following an eruption and then decline toward normal values over several years. Since both ^{3}He and heat are derived from magma, the observations from chronic plumes alone suggest that helium is extracted more efficiently than heat. Helium is soluble in magma although bubbles of gas will exsolve as the magma decompresses. Once the rock solidifies and cracks, it appears that helium must diffuse very rapidly [*Baker and Lupton*, 1990]. *Lowell and Germanovich* [1995] also argue that ^{3}He will degas rapidly from surface lavas and suggest that ^{3}He release from solidifying intrusions may be delayed because at higher pressures dissolved ^{3}He will partition into the molten interior of the intrusion. If event plumes are formed by lava-seawater interactions, the reason for the low ^{3}He/heat ratios remains unclear. Perhaps the initial release of helium from freshly solidified lavas is delayed as helium diffuses slowly through grains and along grain boundaries toward small cracks in which diffusion rates are much higher.

Mn/heat ratios in event plumes are about an order of magnitude lower than those of high- and low-temperature hydrothermal fluid samples at the seafloor and are also substantially lower than those found in chronic plumes [*Massoth et al.*, 1994, 1995]. *Massoth et al.* [1994] note that the source chemistry of the Cleft event plumes suggest that they may have formed by the release of a preexisting reservoir of diffuse vent fluids. *Massoth et al.* [1995] also note that low Mn/heat ratios are compatible with the release of immature hydrothermal fluids. Mn/heat ratios in plumes formed above lava flows entering the ocean from Kilauea volcano, Hawaii are nearly 2 orders of magnitude lower than those found in event plumes [*Sansone et al.*, 1991]. *Sansone et al.* [1991] suggest that the Mn is extracted very inefficiently from seafloor lavas because of the short reaction time. However, Mn concentrations will also increase substantially with reaction temperature [*Seyfried and Mottl*, 1982]. The reaction temperature for seawater-lava interactions is presumably influenced by the seawater boiling point which increases from ~100°C in shallow waters to nearly 400°C along mid-ocean ridges. The intermediate Mn/heat ratios in event plumes may be a consequence of short reaction times at high temperatures.

Although there is now evidence that the heat content of the largest event plumes may be dominated by surface extrusions [*Butterfield et al.*, 1997], the current understanding of the chemical data is insufficient to determine whether the plumes also include a component of mature hydrothermal fluid. If the fluid expansion mechanism generates only a small portion of event plumes, then the constraints on the volume, porosity, permeability, and temperature structure of the reaction zone and the permeability of the upflow zone can be relaxed substantially. In addition to the two large 1986 and 1987 megaplumes, two smaller chemically homogenous event plumes or enhanced chronic plumes were also detected along the Cleft segment in 1987 and 1989 [*Baker*, 1994]. The 1989 plume was not associated with a surface eruption [*Chadwick and Embley*, 1994] and was about 5% of the size of the 1986 event plume. The rise height was 430 m compared with ~300 m for the normal chronic plumes, suggesting that the heat flux increased by a factor of about 4. Such a plume might have resulted from a relatively modest increase in upflow permeability resulting from either a tectonic or intrusive event.

Acknowledgments. I thank Edward Baker, Lawrence Cathles, Paul Delaney, Robert Lowell, and two anonymous referees for many thorough reviews of earlier versions of this manuscript; Andrzej Anderko and Kenneth Pitzer for providing the computer code to implement their equation of state for H_2O-NaCl; and Edward Baker, David Butterfield, Abdellah Cherkaoui, John Delaney, Deborah Kelley, Marvin Lilley, John Lupton, Gary Massoth, Russell McDuff, and Alex McNabb for helpful discussions. Publication of this work was supported by grant OCE-9629425 from the National Science Foundation.

References

Anderko, A., and K. S. Pitzer, Equation-of-state representation of phase equilibria and volumetric properties of the system NaCl-H_2O above 573 K, *Geochim. Cosmochim. Acta*, *57*, 1657-1680, 1993.

Andrews, J. R., and C. H. Emeleus, Structural aspects of kimberlite dyke and sheet intrusion in south-west Greenland, *Phys. Chem. Earth*, *9*, 43-50, 1975.

Baker, E. T., A 6-year time series of hydrothermal plumes over the Cleft segment of the Juan de Fuca Ridge, *J. Geophys. Res.*, *99*, 4889-4904, 1994.

Baker, E. T., and J. E. Lupton, Changes in submarine hydrothermal ^{3}He/heat ratios as an indicator of magmatic/tectonic activity, *Nature*, *346*, 556-558, 1990.

Baker, E. T., G. J. Massoth, and R. A. Feely, Cataclysmic hydrothermal venting on the Juan de Fuca Ridge, *Nature*, *329*, 149-151, 1987.

Baker, E. T., J. W. Lavelle, R. A. Feely, G. J. Massoth, S. L. Walker, and J. E. Lupton, Episodic venting of hydrothermal fluids from the Juan de Fuca Ridge, *J. Geophys. Res.*, *94*, 9237-9250, 1989.

Baker, E. T., G. J. Massoth, R. A. Feely, R. W. Embley, R. E. Thomson, and B. J. Burd, Hydrothermal event plumes from the CoAxial seafloor eruption site, Juan de Fuca Ridge, *Geophys. Res. Lett.*, *22*, 147-150, 1995.

Baker, E. T., G. J. Massoth, J. E. Lupton, S. E. Walker, D. E. Tennat, C. Wilson, and T. Garfield, Time-series sampling of hydrothermal event plume(s) from the 1996 Gorda Ridge eruption (abstract), *Eos Trans. AGU*, *77* (46), Fall Meeting Suppl., F1, 1996.

Berndt, M. E., W. E. Seyfried Jr., and D. R. Janecky, Plagioclase and epidote buffering of cation ratios in mid-ocean ridge hydrothermal fluids: Experimental results in and near the supercritical region, *Geochim. Cosmochim. Acta*, *53*, 2283-2300, 1989.

Bischoff, J. L., and K. S. Pitzer, Phase relations and adiabats in boiling seafloor geothermal systems, *Earth Planet. Sci. Lett.*, *75*, 327-338, 1985.

Bischoff, J. L., and R. J. Rosenbauer, Salinity variations in submarine hydrothermal systems by layered double-diffusive convection, *J. Geol.*, *97*, 613-623, 1989.

Brandsdóttir, B., and P. Einarsson, Seismic activity associated with the September 1977 deflation of the Krafla central volcano in northeastern Iceland, *J. Volcanol. Geotherm. Res.*, *6*, 197-212, 1979.

Butterfield, D. A., I. R. Jonasson, G. J. Massoth, R. A. Feely, K. K., Roe, R. E. Embley, J. F. Holden, R. E. McDuff, M. D. Lilley, and J. R. Delaney, Seafloor eruptions and evolution of hydrothermal fluid chemistry, *Philos. Trans. R. Soc. London, Ser. A*, *355*, 369-386, 1997.

Caltagirone, J. P., and P. Fabrie, Natural convection in a porous medium at high Rayleigh numbers, I, Darcy's model, *Eur. J. Mech.*, *B8*, 207-227, 1989.

Cann, J. R., and M. R. Strens, Modeling periodic megaplume emission by black smoker systems, *J. Geophys. Res.*, *94*, 12,227-12,237, 1989.

Cann, J. R., M. R. Strens, and A. Rice, A simple magma-driven thermal balance model for the formation of volcanogenic massive sulphides, *Earth Planet. Sci. Lett.*, *76*, 123-134, 1985.

Cathles, L. M., A capless 350°C flow zone model to explain megaplumes, salinity variations, and high-temperature veins in ridge axis hydrothermal systems, *Econ. Geol.*, *88*, 1977-1988, 1993.

Chadwick, W. W., Jr., and R. W. Embley, Lava flows from a mid-1980s submarine eruption on the Cleft segment, Juan de Fuca Ridge., *J. Geophys. Res.*, *99*, 4761-4776, 1994.

Chadwick, W. W., Jr., R. W. Embley, and C. G. Fox, Evidence for volcanic eruption on the southern Juan de Fuca Ridge between 1981 and 1987, *Nature*, *350*, 416-418, 1991.

Chadwick, W. W., Jr., R. W. Embley, and C. G. Fox, SeaBeam depth changes associated with recent lava flows, CoAxial Segment, Juan de Fuca Ridge: Evidence for multiple eruptions between 1981-1993, *Geophys. Res. Lett.*, *22*, 167-170, 1995.

Cowan, J., and J. Cann, Supercritical two-phase separation of hydrothermal fluids in the Troodos ophiolite, *Nature*, *333*, 259-261, 1988.

Delaney, J. R., and R. W. Embley, An October response cruise to the June-July intrusive/eruptive events at the CoAxial segment of the Juan de Fuca Ridge (abstract), *Eos Trans. AGU*, *74* (43), Fall Meeting Suppl., 620, 1993.

Delaney, J. R., D. W. Mogk, and M. J. Mottl, Quartz-cemented breccias from the Mid-Atlantic Ridge: Samples of a high-salinity hydrothermal upflow zone, *J. Geophys. Res.*, *92*, 9175-9192, 1987.

Delaney, P. T., D. D. Pollard, J. I. Ziony, and E. H. McKee, Field relations between dikes and joints: Emplacement processes and paleostress analysis, *J. Geophys. Res.*, *91*, 4920-4938, 1986.

Dziak, R. P., C. G. Fox, and A. E. Schreiner, The June-July 1993 seismoacoustic event at CoAxial segment, Juan de Fuca Ridge: Evidence for a lateral dike injection, *Geophys. Res. Lett.*, *22*, 135-138, 1995.

Einarsson, P., and B. Brandsdóttir, Seismological evidence for lateral magma intrusion during the July 1978 deflation of the Krafla Volcano in NE-Iceland, *J. Geophys.*, *47*, 160-165, 1980.

Elder, J. W., Physical processes in geothermal areas, in *Terrestrial Heat Flow, Geophys. Monogr. Ser.*, vol. 8, edited by W. H. K. Lee, pp. 211-239, AGU, Washington, D.C., 1965.

Elder, J. W., *Geothermal Systems*, 508 pp., Academic, San Diego, Calif., 1981.

Embley, R. W., and W. W. Chadwick Jr., Volcanic and hydrothermal processes associated with a recent phase of seafloor spreading at the northern Cleft segment: Juan de Fuca Ridge, *J. Geophys. Res.*, *99*, 4741-4760, 1994.

Embley, R. W., W. W. Chadwick Jr., I. R. Jonasson, D. A. Butterfield, and E. T. Baker, Initial results of the rapid response to the 1993 CoAxial event: Relationship between hydrothermal and volcanic processes, *Geophys. Res. Lett.*, *22*, 143-146, 1995.

Embley, R. W., R. A. Feely, and J. E. Lupton, Introduction to special section on volcanic and hydrothermal processes on the southern Juan de Fuca Ridge, *J. Geophys. Res.*, *99*, 4735-4740, 1994.

Fornari, D. J., and R. W. Embley, Tectonic and volcanic controls on hydrothermal processes at the mid-ocean ridge: An overview based on near-bottom and submersible studies, in *Seafloor Hydrothermal Systems: Physical, Chemical, Biological, and Geological Interactions, Geophys. Monogr. Ser.*, vol. 91, edited by S. E. Humphris, R. A. Zierenberg, L. S. Mullineaux, and R. E. Thomson, pp. 1-46, AGU, Washington, D.C., 1995.

Fox, C. G., W. E. Radford, R. P. Dziak, T.-K. Lau, H. Matsumoto, and A. E. Schreiner, Acoustic detection of a seafloor spreading episode on the Juan de Fuca Ridge using military hydrophone arrays, *Geophys. Res. Lett.*, *22*, 131-134, 1995.

Gamo, T., H. Sakai, J. Ishibashi, E. Nakayama, K. Isshiki, H. Matsuura, K. Shitashima, K. Takeuchi, and S. Ohta, Hydrothermal plumes in the eastern Manus Basin, Bismarck Sea: CH_4, Mn, Al and pH anomalies, *Deep Sea Res.*, *40*, 2335-2349, 1993.

Germanovich, L. N., and R. P. Lowell, The mechanism of phreatic eruptions, *J. Geophys. Res.*, *100*, 8417-8434, 1995.

Gillis, K. M., Mineralogical constraints on the magma - hydrothermal transition in oceanic hydrothermal systems (abstract), *Eos Trans. AGU*, *75* (44), Fall Meeting Suppl., 649, 1994.

Gillis, K. M., and P. T. Robinson, Patterns and processes of alteration in the lavas and dykes of the Troodos ophiolite, Cyprus, *J. Geophys. Res.*, *95*, 21,523-21,548, 1990.

Gillis, K. M., G. Thompson, and D. S. Kelley, A view of the lower crustal component of hydrothermal systems at the Mid-Atlantic Ridge, *J. Geophys. Res.*, *98*, 19,597-19,619, 1993.

Goldfarb, M. S., and J. R. Delaney, Response of two-phase fluids to fracture configurations within submarine hydrothermal systems, *J. Geophys. Res.*, *93*, 4585-4594, 1988.

Grant, M. A., I. G. Donaldson, and P. F. Bixley, *Geothermal Reservoir Engineering*, 369 pp., Academic, San Diego, Calif., 1982.

Grigull, U., J. Straub, and P. Schiebener, *Steam Tables in SI-Units*, 2nd ed., 89 pp., Springer-Verlag, 1984.

Kelley, D. S., and J. Malpas, Melt-fluid evolution in gabbroic rocks from Hess Deep, *Proc. Ocean Drill. Program Sci. Results*, *147*, 213-226, 1996.

Kelley, D. S., and P. T. Robinson, Development of a brine-dominated hydrothermal system at temperatures of 400-500°C in the upper level plutonic sequence, Troodos ophiolite, Cyprus, *Geochim. Cosmochim. Acta*, *54*, 653-661, 1990.

Kelley, D. S., K. M. Gillis, and G. Thompson, Fluid evolution in submarine magma-hydrothermal systems at the Mid-Atlantic Ridge, *J. Geophys. Res.*, *98*, 15,579-19,596, 1993.

Klein, F. W., R. Y. Koyanagi, J. S. Nakata, and W. R. Tanigawa, The seismicity of Kilauea's magma system, in *Volcanism in Hawaii, U.S. Geol. Surv. Prof. Pap.*, *1350*, 1019-1186 1987.

Lavelle, J. W., The initial rise of a hydrothermal plume from a line segment source - Results from a three-dimensional numerical model, *Geophys. Res. Lett.*, *22*, 159-162, 1995.

Lister, C. R. B., On the penetration of water into hot rock, *Geophys. J. R. Astron. Soc.*, *39*, 465-509, 1974.

Lister, C. R. B., The basic physics of water penetration into hot rocks, in *Hydrothermal Processes at Seafloor Spreading Centers*, edited by P. A. Rona, K. Bostrom, L. Laubier, and K. L. Smith, Jr., pp. 141-168, Plenum, New York, 1983.

Lowell, R. P., and L. N. Germanovich, On a mechanism for the formation of megaplumes at ocean ridge axes (abstract), *Eos Trans. AGU*, *74* (43), Fall Meeting Suppl., 243, 1993.

Lowell, R. P., and L. N. Germanovich, On the temporal evolution of high-temperature hydrothermal systems at ocean ridge crests, *J. Geophys. Res.*, *99*, 565-575, 1994.

Lowell, R. P., and L. N. Germanovich, Dike injection and the formation of megaplumes at ocean ridges, *Science*, *267*, 1804-1807, 1995.

Lowell, R. P., P. Van Cappellen, and L. N. Germanovich, Silica precipitation in fractures and the evolution of permeability in hydrothermal upflow zones, *Science*, *260*, 192-194, 1993.

Lupton, J. E., E. T. Baker, and G. J. Massoth, Vertical ^{3}He/heat ratios in submarine hydrothermal systems: Evidence from two plumes over the Juan de Fuca Ridge, *Nature, 337*, 161-164, 1989.

Lupton, J. E., E. T. Baker, G. J. Massoth, R. E. Thomson, B. J. Burd, D. A. Butterfield, R. W. Embley, and G. A. Cannon, Variations in water-column ^{3}He/heat ratios associated with the 1993 CoAxial event, Juan de Fuca Ridge, *Geophys. Res. Lett., 22*, 155-158, 1995.

Massoth, G. J., E. T. Baker, J. E. Lupton, R. A. Feely, D. A. Butterfield, K. L. Von Damm, K. K. Roe, and G. T. Lebon, Temporal and spatial variability of hydrothermal manganese and iron at Cleft segment, Juan de Fuca Ridge, *J. Geophys. Res., 99*, 4905-4923, 1994.

Massoth, G. J., E. T. Baker, R. A. Feely, D. A. Butterfield, R. E. Embley, J. E. Lupton, R. E. Thomson, and G. A. Cannon, Observations of manganese and iron at the CoAxial seafloor eruption site, Juan de Fuca Ridge, *Geophys. Res. Lett., 22*, 151-154, 1995.

McNabb, A., and J. Fenner, Thermohaline convection beneath the ocean floor, in *Proceedings of the CSIRO/DSIR Seminar on Convective Flows in Porous Media*, pp. 157-162, Department of Scientific and Industrial Research, Wellington, New Zealand, 1985.

Middleton, G. V., and J. B. Southard, *Mechanics of Sediment Movement*, Soc. for Sediment. Geol., Tulsa, Oklahoma, 1984.

Nehlig, P., Salinity of oceanic hydrothermal fluids: A fluid inclusion study, *Earth Planet. Sci. Lett., 102*, 310-325, 1991.

Nehlig, P., Interactions between magma chambers and hydrothermal systems: Oceanic and ophiolitic constraints, *J. Geophys. Res., 98*, 19,621-19,633, 1993.

Nehlig, P., Fracture and permeability analysis in magma-hydrothermal transition zones in the Samail ophiolite (Oman), *J. Geophys. Res., 99*, 589-601, 1994.

Nehlig, P., and T. Juteau, Deep crustal seawater penetration and circulation at ocean ridges: Evidence from the Oman ophiolite, *Mar. Geol., 84*, 209-228, 1988.

Nojiri, Y., J. Ishibashi, T. Kawai, A. Otsuki, and H. Sakai, Hydrothermal plumes along the North Fiji Basin spreading axis, *Nature, 342*, 667-670, 1989.

Patankar, S. V., *Numerical Heat Transfer and Fluid Flow*, 153 pp., Hemisphere, Washington, D.C., 1980.

Richardson, C. J., J. R. Cann, H. G. Richards, and J. G. Cowan, Metal-depleted root zones of the Troodos ore-forming hydrothermal systems, Cyprus, *Earth Planet. Sci. Lett., 84*, 243-253, 1987.

Rogers, R. D., and D. K. Bird, Fracture propagation associated with dike emplacement at the Skaergaard intrusion, East Greenland, *J. Struct. Geol., 9*, 71-86, 1987.

Rubin, A. M., Dike-induced faulting and graben subsidence in volcanic rift zones, *J. Geophys. Res., 97*, 1839-1858, 1992.

Rubin, A. M., Tensile fracture of rock at high confining pressure: Implications for dike propagation, *J. Geophys. Res., 98*, 15,919-15,935, 1993.

Sansone, F. J., J. A. Resing, G. W. Tribble, P. N. Sedwick, K. M. Kelly, and K. Hon, Lava-seawater interactions at shallow-water submarine lava flows, *Geophys. Res. Lett., 18*, 1731-1734, 1991.

Schlichting, H., *Boundary Layer Theory*, 817 pp., McGraw-Hill, New York, 1979.

Schreiner, A. E., C. G. Fox, and R. P. Dziak, Spectra and magnitudes of T-waves from the 1993 earthquake swarm on the Juan de Fuca Ridge, *Geophys. Res. Lett., 22*, 139-142, 1995.

Seyfried, W. E., Jr., Experimental and theoretical constraints on hydrothermal alteration processes at mid-ocean ridges, *Annu. Rev. Earth Planet. Sci., 15*, 317-335, 1987.

Seyfried, W. E., Jr., and M. J. Mottl, Hydrothermal alteration of basalt by seawater under seawater-dominated conditions, *Geochim. Cosmochim. Acta, 46*, 985-1002, 1982.

Seyfried, W. E., Jr., K. Ding, and M. E. Berndt, Phase equilibria constraints on the chemistry of hot spring fluids at mid-ocean ridges, *Geochim. Cosmochim. Acta, 55*, 3559-3580, 1991.

Stakes, D. S., Oxygen and hydrogen isotope compositions of oceanic plutonic rocks: High-temperature deformation and metamorphism of oceanic layer 3, in Stable Isotope Geochemistry: A tribute to Samuel Epstein, Geochem. Soc., Spec. Publ. 3, 77-90, 1991.

Turner, J. S., *Buoyancy Effects in Fluids*, 367 pp., Cambridge Univ. Press, New York, 1973.

Von Damm, K. L., Systematics and postulated controls on submarine hydrothermal solution chemistry, *J. Geophys. Res., 93*, 4551-4561, 1988.

White, D. E., Characteristics of geothermal reservoirs, in *Geothermal Energy: Resources, Production, Stimulation*, edited by P. Kruger and C. Otte, pp. 69-94, Stanford Univ. Press, Stanford, Calif, 1973.

Wilcock, W. S. D., A model for the formation of megaplumes (abstract), *Eos Trans. AGU, 75* (44), Fall Meeting Suppl., 619, 1994.

Wilcock, W. S. D., and A. McNabb, Estimates of crustal permeability on the Endeavour segment of the Juan de Fuca mid-ocean ridge, *Earth Planet. Sci. Lett., 138*, 83-91, 1995.

W. S. D. Wilcock, School of Oceanography, University of Washington, Box 357940, Seattle, WA 98195. (e-mail: wilcock@ocean.washington.edu)

(Received May 8, 1995; revised January 31, 1997; accepted February 13, 1997.)